

Concepción Foces-Foces,<sup>\*,a</sup> Antonio L. Llamas-Saiz,<sup>a</sup> Cristina Fernández-Castaño,<sup>a</sup> Rosa M<sup>a</sup> Claramunt,<sup>b</sup> Consuelo Escolástico,<sup>b</sup> José Luis Lavandera,<sup>b</sup> María Dolores Santa María,<sup>b</sup> María Luisa Jimeno<sup>c</sup> and José Elguero<sup>c</sup>

<sup>a</sup> Departamento de Cristalografía, Instituto de Química-Física 'Rocasolano', CSIC, Serrano 119, E-28006 Madrid, Spain

<sup>b</sup> Departamento de Química Orgánica y Biología, Facultad de Ciencias, UNED, Ciudad Universitaria, E-28040 Madrid, Spain

<sup>c</sup> Instituto de Química Médica, CSIC, E-28006 Madrid, Spain

The stability of all possible conformers of hexa(pyrazol-1-yl)benzene [(pz)<sub>6</sub>bz], hexakis(3,5-dimethylpyrazol-1-yl)benzene [(dmpz)<sub>6</sub>bz], 1,2,4,5-tetra(pyrazol-1-yl)-3,6-bis(3,5-dimethylpyrazol-1-yl)benzene [(pz)<sub>4</sub>(dmpz)<sub>2</sub>bz] and 1,4-di(pyrazol-1-yl)-2,3,5,6-tetrakis(3,5-dimethylpyrazol-1-yl)benzene [(pz)<sub>2</sub>(dmpz)<sub>4</sub>bz] has been determined by semiempirical AM1 calculations. In all series the absolute minimum corresponds to the conformation where the nitrogen lone pair of consecutive pyrazole rings is alternately oriented to opposite sides of the benzene plane. The case of (pz)<sub>2</sub>(dmpz)<sub>4</sub>bz has been studied by <sup>1</sup>H NMR studies in solution. Three isomers have been identified and all the signals assigned. The slow evolution to other isomers from those found in the solid state has been followed by <sup>1</sup>H NMR spectroscopy thus allowing determination of the barrier to rotation of a (dmpz) substituent ( $\Delta G^\ddagger = 21\text{--}22$  kcal mol<sup>-1</sup>).

## Introduction

In a series of publications related to 'Aromatic propellenes', that is, compounds formed by a periphery of heteroaromatic rings, usually pyrazoles, directly linked to a central benzene core, we have essentially discussed the ground state structures based on X-ray crystallography and semi-empirical calculations.<sup>1-7</sup> Only in the last publication<sup>7</sup> did we use dynamic HPLC (DHPLC) to determine the rotational barrier of hexakis(3,5-dimethylpyrazol-1-yl)benzene [(dmpz)<sub>6</sub>bz].

## Results and discussion

### Semiempirical calculations

The stability of all conformers of (pz)<sub>6</sub>bz, (dmpz)<sub>6</sub>bz, (pz)<sub>4</sub>(dmpz)<sub>2</sub>bz and (pz)<sub>2</sub>(dmpz)<sub>4</sub>bz that can be obtained when the pyrazole rings (pz or dmpz) are twisted by 180° has been analysed by semiempirical calculations at the AM1 level.<sup>8</sup> Figs. 1 and 2 represent the eight possible conformers for the (pz)<sub>6</sub>bz **a** and (dmpz)<sub>6</sub>bz **b** derivatives (one of them, **3**, being chiral regardless of the values of the torsion angles of the peripheral rings) together with their interconversion paths, which means only one pz (circle) or dmpz (square) 'flip' at the same time. Analogously, Figs. 3 and 4 show the fourteen conformers (six of them being chiral, **3-6**, **10** and **12**) for the (pz)<sub>4</sub>(dmpz)<sub>2</sub>bz **c** and (pz)<sub>2</sub>(dmpz)<sub>4</sub>bz **d** derivatives. The heats of formation (in kcal mol<sup>-1</sup>)<sup>‡</sup> for all up-down conformers and the number of interactions for each conformer, *i.e.* two contiguous pz or dmpz rings with the nitrogen lone pair located at the same side of the benzene plane, are reported in Tables 1 and 2. A more detailed description for compounds of series **a**, **b** and **c** has been given elsewhere,<sup>1-3,7</sup> therefore, the conformational study of **d** will be analysed here, together with a recalculation of the (dmpz)<sub>6</sub>bz **b** case in order to make the computational criteria homogeneous (see Experimental section).

† For Part 7, see ref. 7.

‡ 1 cal = 4.184 J.

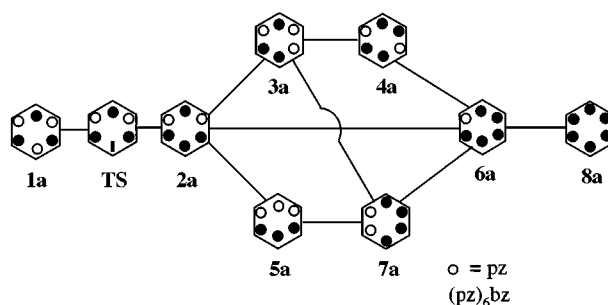


Fig. 1 Eight isomers of (pz)<sub>6</sub>bz; note that isomer **3a** is a mixture of two enantiomers

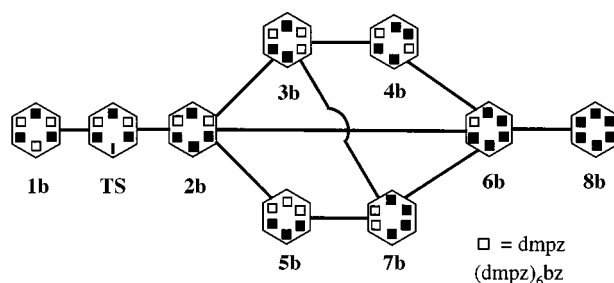


Fig. 2 Eight isomers of (dmpz)<sub>6</sub>bz; note that isomer **3b** is a mixture of two enantiomers

The variation of the relative energies for the eight up-down conformers has the same sequence in (pz)<sub>6</sub>bz and (dmpz)<sub>6</sub>bz (Table 1), although the greater influence of the *uuu* interaction in making conformers more unstable is clear in the latter case, in particular for **6b**.

In (pz)<sub>2</sub>(dmpz)<sub>4</sub>bz (Fig. 4 and Table 2) there are two global minima that correspond to conformer **1** with *C<sub>i</sub>* and *C<sub>2</sub>* point group symmetries. The energy of the conformers increases as the number of pyrazoles (pz or dmpz) with the same orientation increases, *i.e.* increases with the numbers of *uu* or *dd* inter-

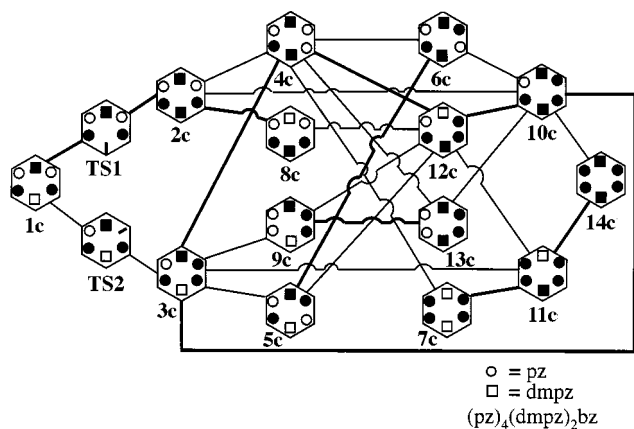


Fig. 3 Fourteen isomers of  $(\text{pz})_4(\text{dmpz})_2\text{bz}$ ; note that isomers 3c–6c, 10c and 12c are mixtures of two enantiomers

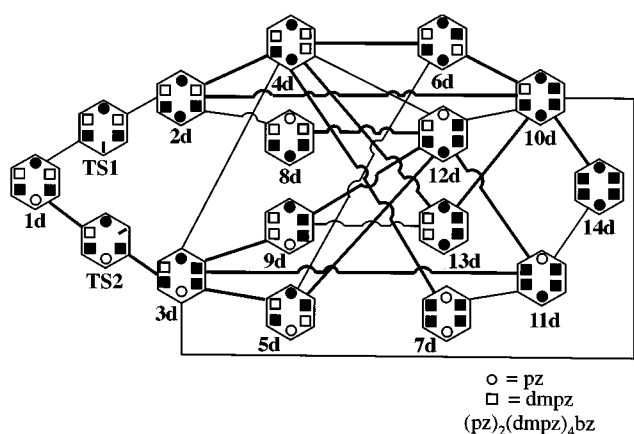


Fig. 4 Fourteen isomers of  $(\text{pz})_2(\text{dmpz})_4\text{bz}$ ; note that isomers 3d–6d, 10d and 12d are mixtures of two enantiomers

actions. However, some differences arise when comparing the present results with those for  $(\text{pz})_4(\text{dmpz})_2\text{bz}$  (Fig. 3 and Table 2). In this compound, all conformers with two interactions (2c–7c) have approximately the same energy, while in the present study the stability of these conformers mainly depends on the dmpz pairs being equally oriented (5d, 6d < 4d < 2d, 3d < 7d). The transition states from 1d to 2d (TS1) or 1d to 3d (TS2), which correspond to a total optimization of the geometry after making the C–C–N–N torsion angle equal to 0° for a pz or a dmpz substituent, have also been calculated (Table 2). At the molecular level, the main difference between the transition states is due to the highest deviation of the N atom bonded to the central benzene ring with regard to the benzene plane.

**Static aspects: relative heats of formation of the different conformers.** We have used several empirical models to discuss the  $\delta\Delta H$  (kcal mol<sup>-1</sup>) values of Tables 1 and 2.<sup>1–3</sup> Here we will use the model given in ref. 3, in which  $\delta\Delta H$  can be broken down into a sum of terms in *uu* and *uuu* [eqns. (1)–(4)]. This model

$$(\text{pz})_6\text{bz} \text{ a} \quad \delta\Delta H = 0.91 \pm 0.05 (uu) + 0.41 \pm 0.07 (uuu) \\ n = 8, r^2 = 0.998 \quad (1)$$

$$(\text{dmpz})_6\text{bz} \text{ b} \quad \delta\Delta H = 0.92 \pm 0.13 (uu) + 0.95 \pm 0.18 (uuu) \\ n = 8, r^2 = 0.993 \quad (2)$$

$$(\text{pz})_4(\text{dmpz})_2\text{bz} \text{ c} \quad \delta\Delta H = 1.21 \pm 0.08 (uu) + 0.23 \pm 0.12 (uuu) \\ n = 14, r^2 = 0.993 \quad (3)$$

$$(\text{pz})_2(\text{dmpz})_4\text{bz} \text{ d} \quad \delta\Delta H = 0.76 \pm 0.11 (uu) + 0.78 \pm 0.16 (uuu) \\ n = 14, r^2 = 0.984 \quad (4)$$

Table 1 Results of the AM1 calculations for  $(\text{pz})_6\text{bz}$  (see Fig. 1) and for  $(\text{dmpz})_6\text{bz}$  (see Fig. 2)

Compound	$\delta\Delta H/\text{kcal mol}^{-1}$	Interactions		Pop. (298 K)
		<i>uu</i>	<i>uuu</i>	
1a	0.0	0	0	0.6317
2a	2.2	2	1	0.0986
3a <sup>a</sup>	2.0	2	0	0.1167
4a	2.1	2	0	0.1073
5a	4.2	4	2	0.0182
6a	4.9	4	3	0.0101
7a	4.3	4	2	0.0167
8a	8.1	6	6	0.0007
1b	0.0	0	0	0.6979
2b	2.8	2	1	0.0656
3b <sup>a</sup>	2.0	2	0	0.1290
4b	2.5	2	0	0.0846
5b	4.7	4	2	0.0131
6b	7.1	4	3	0.0017
7b	5.3	4	2	0.0080
8b	11.3	6	6	0.0001

<sup>a</sup> Racemic. TS (1a→2a),  $\delta\Delta H = 12.6$  kcal mol<sup>-1</sup>. TS (1b→2b),  $\delta\Delta H = 21.2$  kcal mol<sup>-1</sup>.

Table 2 Results of the AM1 calculations for  $(\text{pz})_4(\text{dmpz})_2\text{bz}$  (see Fig. 3) and for  $(\text{pz})_2(\text{dmpz})_4\text{bz}$  (see Fig. 4)

Compound	$\delta\Delta H/\text{kcal mol}^{-1}$	Interactions		Pop. (298 K)
		<i>uu</i>	<i>uuu</i>	
1c	0.0	0	0	0.5957
2c	2.8	2	1	0.0560
3c <sup>a</sup>	2.5	2	1	0.0722
4c <sup>a</sup>	2.6	2	0	0.0663
5c <sup>a</sup>	2.7	2	0	0.0610
6c <sup>a</sup>	3.0	2	0	0.0473
7c	2.9	2	0	0.0515
8c	4.7	4	2	0.0113
9c	4.5	4	2	0.0133
10c <sup>a</sup>	5.7	4	3	0.0048
11c	5.3	4	3	0.0068
12c <sup>a</sup>	5.3	4	2	0.0068
13c	5.3	4	2	0.0068
14c	9.2	6	6	0.0002
1d	0.0	0	0	0.4140
2d	2.3	2	1	0.0594
3d <sup>a</sup>	2.3	2	1	0.0594
4d <sup>a</sup>	1.8	2	0	0.0906
5d <sup>a</sup>	1.2	2	0	0.1503
6d <sup>a</sup>	1.3	2	0	0.1381
7d	3.0	2	0	0.0328
8d	4.6	4	2	0.0085
9d	3.8	4	2	0.0167
10d <sup>a</sup>	5.1	4	3	0.0056
11d	6.2	4	3	0.0022
12d <sup>a</sup>	4.5	4	2	0.0093
13d	4.1	4	2	0.0130
14d	9.5	6	6	0.0001

<sup>a</sup> Racemic. TS1 (1c→2c),  $\delta\Delta H = 23.1$  kcal mol<sup>-1</sup>. TS2 (1c→3c),  $\delta\Delta H = 11.2$  kcal mol<sup>-1</sup>. TS1 (1d→2d),  $\delta\Delta H = 11.2$  kcal mol<sup>-1</sup>. TS2 (1d→3d),  $\delta\Delta H = 22.1$  kcal mol<sup>-1</sup>.

does not differentiate, for mixed derivatives **c** and **d**, between adjacent pzs and dmpzs.

**Dynamic aspects: rotational barriers.** The most important conclusion of the AM1 calculations for the NMR studies in solution is that these compounds present two types of barriers. The first one corresponds to the rotation of a pz ring and has an activation barrier of 11.2–12.6 kcal mol<sup>-1</sup> (Tables 1 and 2). The second one corresponds to the rotation of a dmpz and has an activation barrier of 21.2–23.1 kcal mol<sup>-1</sup> (Tables 1 and 2). The pz or dmpz which rotates is represented in Figs. 1–4 by a line.

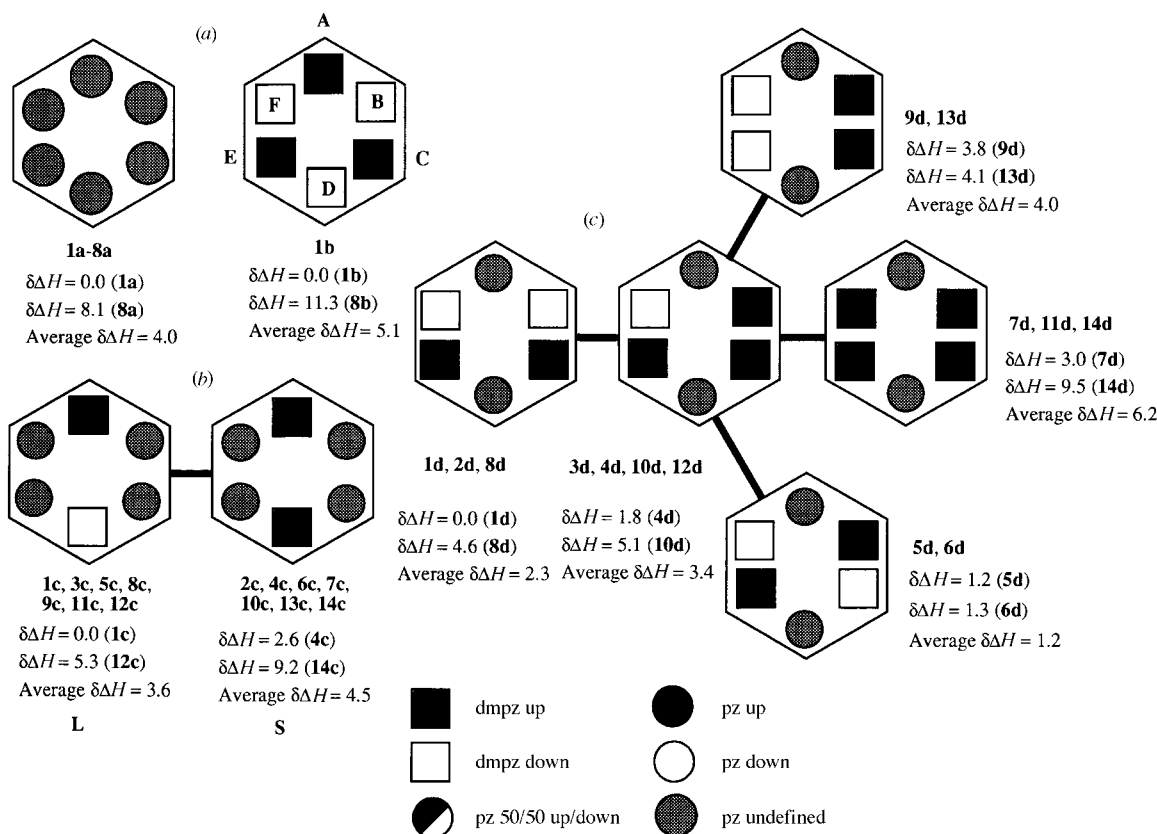


**Fig. 5** Notation used to describe propellenes in the case of (a)  $(\text{pz})_6\text{bz}$  **a** and  $(\text{dmpz})_6\text{bz}$  **b**. The six dmpz substituents of positions 1–6 of **b** are A, B, C, D, E and F. (b) The two isomers of  $(\text{pz})_4(\text{dmpz})_2\text{bz}$  **c**. (c) The five isomers of  $(\text{pz})_2(\text{dmpz})_4\text{bz}$  **d**.

The fact that the first barrier is very low justifies the observation in the NMR spectra of narrow average signals at usual temperatures; the second barrier is large enough to observe narrow signals for each isomer in the NMR spectra for the usual NMR temperatures (250–400 K). As a first approximation, the six barriers reported in Tables 1 and 2 can be decomposed into a sum of two terms, one for each adjacent pyrazole. For rotation of pz, the contributions are pz 6.1, dmpz 5.4 kcal mol<sup>-1</sup> and for rotation of dmpz, they are 11.6 and 10.6 kcal mol<sup>-1</sup>, roughly twice as much. Thus, an adjacent pz group seems to produce more steric hindrance than dmpz, which may seem paradoxical, but one has to consider the structure of the transition states in which the 3,5-substituents of the pyrazole ring in dmpz are far removed from the contact zone in the transition states.

Classical kinetics (isomerization) or DHPLC<sup>7</sup> can be used for studying the rotation of dmpz. In Figs. 1 to 4, a narrow line (low barrier) is used to connect isomers through the 180° rotation of a single pz while a broad line (high barrier) corresponds to single interconversion paths related to a 180° dmpz rotation.

Fig. 5 shows the conformations expected in solution. For  $(\text{pz})_6\text{bz}$  **a**, only one series of signals should be observed and this is actually the case. Fig. 5(a) (grey circles) does not signify that all the conformations will be equally populated; the conformation of lower energy, **1a**, must be predominant but others could be present in significant amounts. For instance, **3a** (2.0 kcal mol<sup>-1</sup> higher in energy, Table 1) has also been isolated in the solid state as a conformational polymorph of **1a**.<sup>2</sup>

For  $(\text{dmpz})_6\text{bz}$  **b**, all isomers could be observed by NMR spectroscopy, but only the most stable were found: **1b** and **2b**, in the ratio 86:14, which corresponds to  $\Delta G_{298} = 1.1$  kcal mol<sup>-1</sup> (in Table 1,  $\delta\Delta H$  2.8 kcal mol<sup>-1</sup>).<sup>1,7</sup>

The mixed compound  $(\text{pz})_4(\text{dmpz})_2\text{bz}$  **c** [Fig. 5(b)] also exhibits polymorphism in the solid state but both polymorphs have the same conformation **1c**. This compound should exist in only two conformations (large, **L** and small, **S**) in solution, which is what was observed: **L/S** = 90:10,  $\Delta G_{298} = 1.3$  kcal mol<sup>-1</sup> (in Table 2,  $\delta\Delta H$  for **1c** and **4c** = 2.6 kcal mol<sup>-1</sup>).<sup>3</sup> The last

compound,  $(\text{pz})_2(\text{dmpz})_4\text{bz}$  **d**, is the most interesting since four conformations are possible [Fig. 5(c)] and its study in solution will be described in detail below. In the solid state, this compound and its inclusion derivatives only exist in the conformation **1d**.<sup>5</sup>

#### NMR study in solution of compound $(\text{dmpz})_6\text{bz}$ **b**

We have studied again the behaviour of this compound because the previous NMR study was carried out in CDCl<sub>3</sub> + CF<sub>3</sub>-CO<sub>2</sub>H and this probably affects the distribution of populations (protonation will change a repulsive *uu* interaction to an attractive *uu+* one).<sup>1</sup> Moreover, the DHPLC study was carried out in water–methanol and the method does not allow identification of the isomers involved.<sup>7</sup> Fig. 2 shows the four ways in which the different dmpzs can be arranged: only one dmpz (six identical dmpzs), **1b** and **8b**; two kinds of dmpzs in a 1:2 ratio (or 2:4), **4b** and **5b**; three kinds of dmpzs in a 1:1:1 ratio (or 2:2:2), **3b** and **7b**; four kinds of dmpzs in a 1:2:2:1 ratio, **2b** and **6b**. The compound previously identified by <sup>1</sup>H NMR spectroscopy belongs to the 1:2:2:1 class and bidimensional experiments proved that its structure was **2b**.

Now (in pure CDCl<sub>3</sub>) we have observed that the initial amount of compound **1b** (only one dmpz) diminishes leading to compound **2b** (four dmpzs) and this last in turn disappears to yield a compound showing the 1:1:1 pattern to which we have assigned the structure **3b**. At equilibrium, the relative amounts are 44% **1b**, 12% **2b** (or **4b**) and 44% **3b**. The <sup>13</sup>C NMR results proved that the two major isomers (in a 1:1 relative ratio) are **1b** and **3b** (see Table S1, Supplementary Material).‡

‡ The following data has been deposited as Supplementary Material (suppl. no. 57298, 4 pp.) at the British Library. <sup>1</sup>H and <sup>13</sup>C NMR chemical shifts of  $(\text{dmpz})_6\text{bz}$  **b** isomers in CDCl<sub>3</sub> (Table S1); <sup>13</sup>C NMR chemical shifts of the three isomers of  $(\text{pz})_2(\text{dmpz})_4\text{bz}$  **d** in CDCl<sub>3</sub> (Table S1). LSR\* experiments with compound  $(\text{pz})_2(\text{dmpz})_4\text{bz}$  **d** in CDCl<sub>3</sub> (Table S2). AM1 calculated dipole moments of all isomers (Table S3). For details, of the Supplementary Publications Scheme, see 'Instructions for Authors', *J. Chem. Soc., Perkin Trans. 2*, 1997, Issue 1.

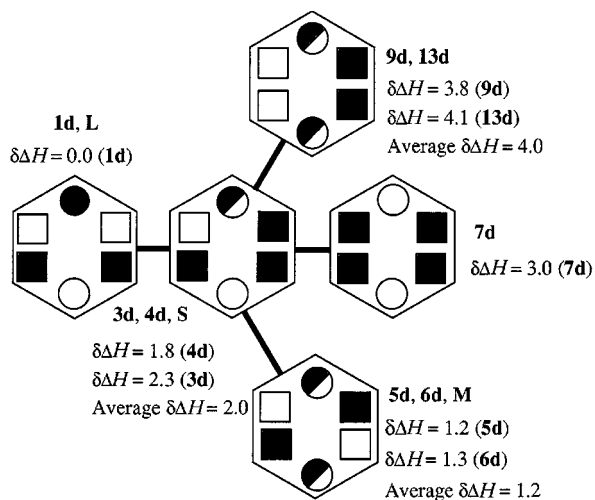


**Fig. 6** Different isomers of  $(pz)_2(dmpz)_4bz$  **d** taking into account the orientation of the four dmpz substituents

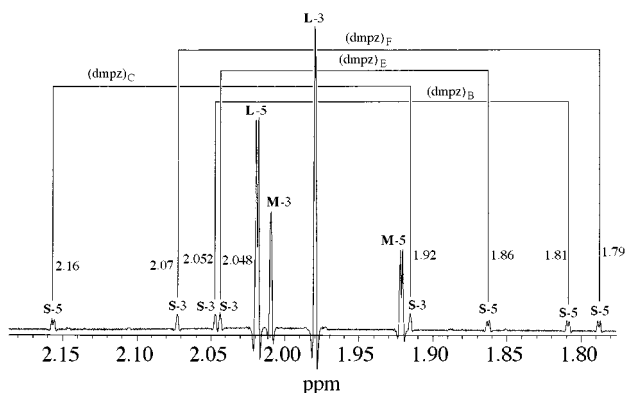


**Fig. 7** Methyl part of the  $^1H$  NMR spectrum (500 MHz) of  $(pz)_2(dmpz)_4bz$  **d** in  $CDCl_3$

#### NMR study in solution of compound $(pz)_2(dmpz)_4bz$ **d**

**Assignment of isomers.** The crystal structure of compound **1d** was determined from a given crystallization batch (dichloromethane–hexane). The remaining crystals (identical appearance) were used for the NMR experiments. When the  $^1H$  NMR spectrum of a solution of **1d** in  $CDCl_3$  was recorded soon after preparation, only the signals corresponding to **1d** were observed; if the solution was allowed to evolve for several days at room temperature, then an equilibrium mixture of **1d** (63%, large **L**) and two other isomers (23 and 14%) was obtained (evaporation of the solution yield crystals of **1d** pure). The first problem was to determine the structure of the medium (**M**) and small (**S**) isomers.

The conformation of the pzs residues should depend mostly on the destabilizing *uu* and *uuu* situations. In the case of the initial product (**L**), conformation **1d** complies with both of these requirements (see Table 2). The second product in the high-barrier path should have a pzs down (because it is surrounded by two dmpz up), the other product has been represented as a 50:50 up–down taking into account its neighbours, that is, conformers **3d** ( $\delta\Delta H = 2.3$  kcal mol $^{-1}$ , Table 2) and **4d** (or an enantiomer,  $\delta\Delta H = 1.8$  kcal mol $^{-1}$ , Table 2). The rest of Fig. 6 is self-explanatory.

The spectrum of compound **d** [ $(pz)_2(dmpz)_4bz$ ] was recorded several times at 400 and 500 MHz. Fig. 7 shows the section corresponding to the 12 methyl signals of the dmpzs. It is easy to differentiate the signals corresponding to the 3- and 5-positions of the pyrazole ring since only the 5-methyl groups (**L**-5, **M**-5 and **S**-5) are coupled with the H4 proton. It is easy to identify the methyl signals of **L** and **M** taking into account their relative intensities. To assign the methyl signals of **S** to individual dmpzs a series of COSY (through H4) and NOESY

**Table 3** Experimental and calculated populations of propellenes **a–d** at 298 K

Compound	Experimental result	AM1 calculated populations
$(pz)_6bz$ <b>a</b>	No data	Averaged mixture rich in <b>1a</b>
$(dmpz)_6bz$ <b>b</b>	44% <b>1b</b> /12% <b>4b</b> or <b>2b</b> / 44% <b>3b</b>	70% <b>1b</b> /8% <b>4b</b> /13% <b>3b</b>
$(pz)_4(dmpz)_2bz$ <b>c</b>	90% <b>L</b> /10% <b>S</b>	77% <b>L</b> <sup>a</sup> /23% <b>S</b> <sup>b</sup>
$(pz)_2(dmpz)_4bz$ <b>d</b>	63% <b>L</b> /23% <b>M</b> /14% <b>S</b>	71% <b>L</b> <sup>c</sup> /25% <b>M</b> <sup>d</sup> /5% <b>S</b> <sup>e</sup>

<sup>a</sup> **1c**, **3c**, **5c**, **8c**, **9c**, **11c**, **12c**. <sup>b</sup> **2c**, **4c**, **6c**, **7c**, **10c**, **13c**, **14c**. <sup>c</sup> **1d**, **2d**, **8d** (48%). <sup>d</sup> **3d**, **4d**, **10d**, **12d** (16.5%). <sup>e</sup> **7d**, **11d**, **14d** (3.5%).

experiments were carried out. Similar experiments involving the protons of the pzs allowed us to determine all the information required to develop Fig. 8.

We have also carried out NOE selective experiments, one of the most significant being the one between the signals at 1.79 ppm (5-methyl of ring B) and 1.86 ppm (5-methyl of ring C) since it proves simultaneously that ring B and C are adjacent and also that they are both up (or down). The other proximities of the **S** component were established using the same procedure; the only assumption we made is to assign **A** to the upper pzs by analogy of its  $^1H$  chemical shifts with those of **M**, and **D** to lower pzs by analogy with those of **L**. The corresponding  $^{13}C$  NMR data are reported in Table S1 of the Supplementary Material.

These experiments established the sequence **1d**→**3d**, **4d**→**5d**, **6d** for the evolution of isomers with time. The corresponding Boltzmann distribution is  $\delta\Delta G_{298} = 0.0, 0.9$  and  $0.6$  kcal mol $^{-1}$  which should be compared with 0.0 (**L**), 2.0 (**S**) and 1.2 kcal mol $^{-1}$  (**M**) (Fig. 6).

We have also carried out a  $^1H$  NMR experiment by adding a chiral shift reagent (LSR\*, Aldrich 'Resolve') to an equilibrated mixture (15 days) of **L**, **M** and **S** isomers. The results (see Supplementary Material, Table S2) are interesting but difficult to rationalize: (i) the splitting (characteristic of a racemic) affects only the dmpz signals not those of pzs; (ii) the splitting affects the three isomers and it decreases in the order **S** > **M** > **L**; (iii) the slopes (sensitivity of the signal to the LSR\*) decrease in the order: position 5 > position 3 > position 4.

In summary, with regard to LSR\* all the three isomers appear as racemic compounds, probably due either to their helical conformation or to asymmetric associations.

**Calculation of the barrier.** A classical kinetic experiment was carried out using  $^1H$  NMR spectroscopy (at 500 MHz) to follow the evolution of the intensities of the signals associated with **L**, **M** and **S**. From the kinetic results (see Experimental section), the activation barriers between the three isomers have been determined through the equation  $\Delta G^\ddagger = 4.57 T [10.32 + \log(T/k)]$ . The actual values (for  $T = 298$  K) are: from **L** to **S**, 22.4 kcal mol $^{-1}$ ; from **S** (which lies 0.9 kcal mol $^{-1}$  higher than **L**) to **M** (which lies 0.6 kcal mol $^{-1}$  higher than **L**), 21.1 kcal mol $^{-1}$ . The calculated barrier (Table 2, TS2, **1d**→**3d**, 22.1 kcal mol $^{-1}$ ) agrees with the experimental value (22.4 kcal mol $^{-1}$ ).

## Discussion

We now have all the necessary elements for discussing the conformation of propellenes **a–d** if we combine judiciously the experimental results and the AM1 calculations. The agreement between the experimental and calculated values for the activation barriers is entirely satisfactory.

Concerning the energies, the situation can be summarized by Table 3. These calculations were based on the empirical observation that approximately  $\Delta H_{\text{calc}} = 0.5\Delta G_{298}$ . We have halved the  $\Delta H_{\text{calc}}$  values of Tables 1 and 2, calculated the corresponding populations at 298 K (Pop. 298) and reported them in the

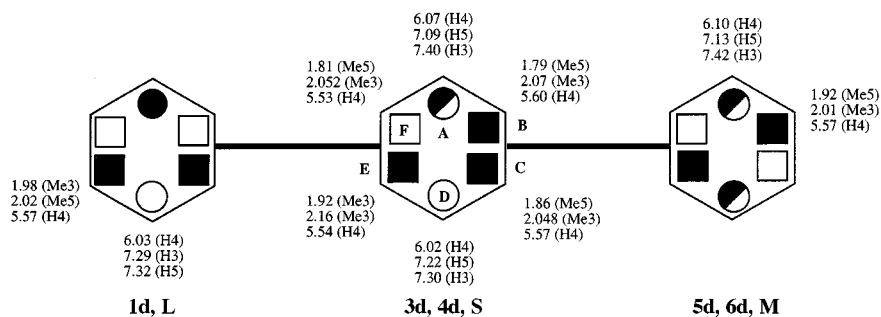


Fig. 8 Assignment of the  $^1\text{H}$  NMR spectrum of  $(\text{pz})_2(\text{dmpz})_4\text{bz}$  **d** in  $\text{CDCl}_3$  to isomers **L**, **S** and **M**

Table 4 Kinetic results for compound  $(\text{pz})_2(\text{dmpz})_4\text{bz}$  **d**

Spectra	Time/s	Integration <sup>a</sup>		
		L	M	S
1	0	91.4	2.8	6.8
2	60	88.8	3.3	7.7
3	1220	68.4	19.2	11.9
4	2560	62.5	22.9	13.8

<sup>a</sup> Isomer **L**  $X_0 = 0$ ,  $Y_0 = 60.98$ ,  $t_1 = 863.93$ ,  $A_1 = 30.15$ ,  $\chi^2 = 0.174$  24; Isomer **M**  $X_0 = 0$ ,  $Y_0 = 76.08$ ,  $t_1 = 817.80$ ,  $A_1 = 21.60$ ,  $\chi^2 = 0.555$  87; Isomer **S**  $X_0 = 0$ ,  $Y_0 = 85.36$ ,  $t_1 = 1174.30$ ,  $A_1 = 7.59$ ,  $\chi^2 = 0.139$  68.

right side of these Tables. The agreement is acceptable, although the fact that the starting isomer (**1**) is experimentally less stable (**1b**, **Lc**, **Ld**) than has been calculated may be related to the fact that this conformer has no dipole moment (see Table S2, Supplementary Material), which probably disfavors it in a solvent like  $\text{CDCl}_3$  with regard to other isomers like **2** (average  $\mu = 3.1$  D) and **3** (average  $\mu = 1.6$  D).

## Experimental

### Semiempirical calculations

The semiempirical calculations were performed using the AM1 model for the parametrization of the Hamiltonian and with the MOPAC<sup>8</sup> 6.0 set of programs running on a DEC3000-300X workstation. The only geometrical restriction imposed was the planarity of the aromatic rings and the corresponding torsion angle in the case of the transition states. Several starting points were employed for each up-down conformation in order to avoid local minima.

### NMR spectroscopy

The  $^1\text{H}$  NMR spectra were recorded on a Varian Unity 500 spectrometer working at 499.84 MHz (Fig. 7) and on a Bruker Avance DRX-400 spectrometer working at 400.13 MHz.  $^{13}\text{C}$  NMR spectra were recorded on a Bruker Avance DRX-400 spectrometer working at 100.62 MHz. The experimental conditions and the two-dimensional experiments are those described in ref. 9. To establish the conformation of compounds **b** and **d**

we have recorded on a Bruker Avance DRX-400 spectrometer the following NMR experiments with pulsed field gradients: NOE selective, NOESY, COSY and HMQC.

### Kinetic experiments

The spectra of  $(\text{pz})_2(\text{dmpz})_4\text{bz}$  **d** were recorded at 25 °C. Four spectra were recorded in  $\text{CDCl}_3$  at 0, 60, 1220 and 2560 s. In the fitting procedure, a short lapse of time to record the first spectrum was assumed. The data (Table 4) were treated as a first-order reaction using an exponential fitting to an equation of the form  $Y = Y_0 + A_1 \exp[-(X + X_0)/t_1]$ .

## Acknowledgements

We thank the CICYT (Spain) for financial support (project numbers PB93-0125 and PB93-0197-C02).

## References

- C. Foces-Foces, A. L. Llamas-Saiz, R. M. Claramunt, N. Jagerovic, M. L. Jimeno and J. Elguero, *J. Chem. Soc., Perkin Trans. 2*, 1995, 1359.
- C. Foces-Foces, A. L. Llamas-Saiz, C. Escolástico, R. M. Claramunt and J. Elguero, *J. Phys. Org. Chem.*, 1996, **9**, 137.
- C. Foces-Foces, C. Fernández-Castaño, R. M. Claramunt, C. Escolástico and J. Elguero, *J. Phys. Org. Chem.*, 1996, **9**, 717.
- P. Cornago, C. Escolástico, M. D. Santa María, R. M. Claramunt, C. Fernández-Castaño, C. Foces-Foces, J.-P. Fayet and J. Elguero, *Tetrahedron*, 1996, **52**, 11 075.
- C. Foces-Foces, C. Fernández-Castaño, R. M. Claramunt, C. Escolástico and J. Elguero, submitted for publication in *J. Inclusion Phenom. Mol. Recogn.*
- C. Fernández-Castaño, C. Foces-Foces, F. H. Cano, R. M. Claramunt, C. Escolástico, A. Fruchier and J. Elguero, *New J. Chem.*, 1997, **21**, 195.
- J. L. Lavandera, R. M. Claramunt, C. Escolástico, M. D. Santa María and J. Elguero, *Bull. Soc. Chim. Belg.*, in the press.
- J. J. P. Stewart, MOPAC6.0, Frank J. Seiler Research Laboratory, United States Air Force Academy, CO 80840, USA, 1990.
- S. Braun, H.-O. Kalinowski and S. Berger, *100 and More Basic NMR Experiments*, VCH, New York, 1996.

Paper 7/04257D

Received 17th June 1997

Accepted 24th July 1997